AMERICAN JOURNAL OF
CHEMISTRY AND PHARMACY (AJCP)
ISSN: 2834-0116 (ONLINE)
VOLUME 2 ISSUE 1 (2023)
PUBLISHED BY
E-PALLI PUBLISHERS, DELAWARE, USA

American Journal of Chemistry and Pharmacy (AJCP)

Volume 2 Issue 1, Year 2023
ISSN: 2834-0116 (Online)
DOI: https://doi.org/10.54536/ajcp.v2i1.1293
https://journals.e-palli.com/home/index.php/ajcp

Synthesis and Characterization of *Alpinia calcarata* Loaded Nanoparticles to Control Hyperglycemia

B.S. Wanniarachchi[1], P.G.U. Chathuranga[1], P.H.U.W. De Silva[1], B.M. Jayawardena[1*]

Article Information

Received: February 12, 2023

Accepted: March 02, 2023

Published: March 10, 2023

Keywords

A.Calcarata, Antidiabetic, BSA Nanoparticles, Citric Acid, Nutraceutical

ABSTRACT

Bovine Serum Albumin (BSA) nanoparticles loaded with the bioactive compounds of *A. calcarata*, which is known to exert its antidiabetic activity through the inhibition of pancreatic enzymes, are a good form of an antidiabetic nutraceutical as they have reduced side effects, protection of active compounds from environmental agents, specific delivery to target sites and prolonged shelf-life. The objective of the present study was to synthesize and characterize *A. calcarata* loaded nanoparticles (ALNP) to be used as a powder form nutraceutical with higher antidiabetic activity. In this study an aqueous *A. calcarata* extract (4.00 mL) was added to BSA (20 mg/mL, 4.00 mL, pH 9) in the presence of citric acid as the cross-linking agent. The ALNP gave an IC50 value of 147 µg/mL, a glucose (5 mM) uptake percentage of 73.09% at a 0.5 mg/mL concentration, a solubility value of 64%, *A. calcarata* loading percentage of 6.66% and *A. calcarata* entrapment efficiency of 87.71%. They had a spherical morphology and uniform size with a particle size of 1030.70 nm, PDI of 0.199 and a zeta potential of 2.57 mV. The UV-Visible absorbance spectra and FT-IR spectra showed that citric acid had caused conformational changes in the protein structure of BSA and that the active compounds were successfully loaded into the synthesized nanoparticles which interacted with the protein matrix via covalent bonds. Therefore, it can be concluded that the synthesized nanoparticles have an antidiabetic effect and the antidiabetic activity of bioactive compounds of the aqueous *A. calcarata* extract become enhanced when loaded onto the nanocarriers.

INTRODUCTION

Diabetes mellitus, the most common non-communicable disease in the world is coined from the Greek word diabetes, meaning to pass through a large discharge of urine and the Latin word mellitus, meaning sweet. It is a general term used to describe a variety of metabolic disturbances, the primary cause of which is chronic hyperglycemia. (Sapra & Bhandari, 2022; Kerner & Brückel, 2014) Type 1 diabetes mellitus (T1DM), type 2 diabetes mellitus (T2DM), 'other' and gestational diabetes mellitus (GDM) are the classifications of diabetes based on etiology and pathology. (Guthrie & Guthrie, 2004)

According to the World Health Organization (WHO), in 2019, diabetes was the ninth leading cause of death and is also responsible for the largest rise in male deaths with an 80% increase since 2000. It is the No.1 cause of kidney failure, adult blindness and lower-limb amputations. Also in 2019, among the US population, 283,000 children and adolescents younger than 20 years suffered from diagnosed diabetes. The 2022 National Diabetes Statistics Report states that currently about 382 million (8.3%) people are affected by diabetes and this number is projected to increase to 552 million (53%) by 2035. (Kharroubi & Darwish, 2015)

Oral antidiabetic drugs that are used in the treatment of diabetes have serious side effects such as hypoglycemia, weight gain, anemia and congestive heart failure. Also, due to their high cost and these side effects, scientists are searching for more effective and safer antidiabetic drugs. Therefore, recently attention has been focused on natural products including food plants, as possible sources of more potent and safer antidiabetic therapy. (Kazeem & Davies, 2016)

Alpinia calcarata Roscoe which belongs to the family Zingiberaceae is a rhizomatous plant that is widely used as a medicinal source in Sri Lanka. Rhizomes of this plant are known as Heen araththa or Katu kikiriya in Sinhala and snap ginger in English. The mature rhizomes are dense and branched with a light to dark brown colour and they are the most important part of this plant, as they are a major part of indigenous medicinal formulation for the treatment of blood impurities, indigestion, throat inflammation, voice improvement and to marinate youthful vigor. The decoction of *Alpinia calcarata* rhizome is widely used to treat respiratory ailments, cough, bronchitis, asthma and arthritis. The ethanolic as well as aqueous extracts of *Alpinia calcarata* rhizomes show antibacterial, antifungal, anthelminthic, anti-inflammatory, antioxidant, anticancer, antinociceptive, gastroprotective, aphrodisiac and antidiabetic effects. This herb is also used as a traditional medicine for stomachache, fever and rheumatism. (Rahman & Islam, 2015)

Analysis of *A.calcarata* Rosc. grown in Sri Lanka has revealed the presence of quercetin, protocatechuic acid, 1,8-cineole, β-pinene, vanillic acid, 4-O-methyl-syringic acid and methyl cinnamate as well as several terpenes and diterpenes as constituents. Novel bis-labdanic diterpenoids such as calcaratarin D and calcaratarin

[1] Department of Chemistry, University of Kelaniya, Sri Lanka
[*] Corresponding author's e-mail: bimali@kln.ac.lk

E have been isolated and identified from its rhizomes, which are known to be a pair of stereoisomers according to spectral evidence. Qualitative phytochemical analysis, of the hot water extract and hot ethanol extract, also revealed the presence of alkaloids, flavonoids, steroid glycosides, polyphenols and tannins in its rhizomes. The relative percentages of water extractable matter and ethanol extractable matter are 18.6-20.5 and 22.6-24.8, respectively. (Rahman & Islam, 2015) The essential oils of rhizomes, roots and leaves when analyzed using capillary GC and GC/MS showed the presence of 18 compounds. The major compound in the leaf and rhizome oils was 1,8-cineole and in the root oil it was α-fenchyl acetate. *A. calcarata*, having such a huge range of phytochemical diversity, has been ensured non-toxic and safe in animal studies. (Arambewela *et al*., 2005)

Scientific studies carried out with the oral administration of the hot ethanolic and hot water extracts of the rhizomes of *A. calcarata* to normoglycemic and streptozotocin-induced diabetic rats have shown hypoglycemic and antihyperglycemic effects, respectively. Both hot water and hot ethanol extracts significantly reduce the blood glucose level, body weight gain, plasma triglyceride and total cholesterol levels as well as improve the glucose tolerance. *Alpinia calcarata* extract exerts its potent antidiabetic activity through the inhibition of intestinal glucose absorption by inhibiting the activity of pancreatic α-amylase and α-glucosidase enzymes. However, the hypoglycemic effect of hot ethanol extract is usually higher than that of hot water extract. Phenolic compounds such as flavonoids, polyphenols and tannins that are present in its rhizomes are known to be responsible for its antidiabetic activity. (Rahman & Islam, 2015; Wasana *et al*., 2021)

Extraction procedures are carried out to separate the medicinally active portions of plant or animal tissues from the inactive or inert components by using selective solvents. (Handa *et al*., 2008) Some of the extraction techniques that can be used to extract the active compounds of the bark of *A.calcarata* are microwave digestion, pressurized water extraction, solvent extraction, decoction water extraction and infusion water extraction. Out of these techniques, the pressurized water extraction has been proven to result in an aqueous extract that is more active than the other. (Wariyapperuma *et al*., 2018)

Unlike the traditional extraction methods that require large volumes of non-environmental friendly organic solvents and is time consuming with low extraction efficiency, pressurized water extraction, which is a green solvent extraction method, is environmentally friendly as it uses minimum or no organic solvent, cheap with shorter extraction time and high extraction efficiency. The analytes extracted using this method are also safe for human consumption, testing and processing as organic solvents are not involved. As water is easily available, non-toxic and can be recycled or disposed with minimal environmental problems, pressurized water extraction has steadily become an efficient and low-cost method of extraction for less-polar organic components. (Teo *et al*., 2010; Jayawardena & Smith, 2010)

"Pressurized hot water" is used to denote the region of condensed phase of water from 100 ℃ to 374 ℃, which is the critical point of water. The density of water remains almost constant over this temperature range so that the pressure effect on the properties of water is minimal. During extraction, moderate pressures such as 15 bar at 200 ℃ and 85 bar at 300 ℃ are needed to keep a condensed phase of water. Under these conditions the dielectric constant of water decreases, and it starts behaving as an organic solvent such as ethanol and methanol, which can then extract organic and non-polar compounds from numerous kinds of matrices. However, if water was used at room temperature and atmospheric pressure, it will not be suitable for the extraction of organic and non-polar compounds, because of its high polarity and high dielectric constant due to its hydrogen bonded structure. (Teo *et al*., 2010)

With the advance of nanotechnology, scientists have developed nanoencapsulation techniques for the targeted release and protection of pharmaceuticals and food bioactive components, so that they can be safely added into formulations and result in maximum bioavailability. Conventional microencapsulation technologies include physical and chemical processes such as spray drying, freeze drying, extrusion, coacervation, liposomes and conventional emulsions. Unlike these methods, nanocarriers could provide more bioavailability through increased surface-to-volume ratios and therefore higher muco-adhesive possibility within the small intestine and higher feasibility of interacting with enzymes and metabolic factors, and also these tiny particles could easily pass through the cell membranes and penetrate into the target cells and release their encapsulated material. (Assadpour & Mahdi Jafari, 2019) In addition, these nanocarriers can also improve the solubility of hydrophobic compounds, such as the active compounds of cinnamon, protect the chemical structure of nutraceuticals from environmental agents such as light, temperature, pH, radicals and oxygen, allow specific delivery to target sites, allow a controlled release of the encapsulated compound, result in reduction of side effects and prolonged shelf-life, and also, they have minimum influence on the appearance of final food products. (Assadpour & Mahdi Jafari, 2019; Paolino *et al*., 2021)

A nanocarrier is a nano-sized system and is scientifically defined in the pharmaceutical area as a particle with a size of a few nm to just below 1000 nm. (Assadpour & Mahdi Jafari, 2019) Nanoparticles fall into the category of colloidal drug delivery system as they behave as a whole unit with respect to its properties and transport mechanism. Several types of nanoparticle systems have been identified such as polymeric nanoparticles, polymeric micelles, solid nanoparticles, lipid-based nanoparticles for example, solid lipid nanoparticles (SLN), nanostructured lipid carriers (NLC) and lipid drug conjugate (LDC), liposomes, inorganic nanoparticles, dendrimers, magnetic

nanoparticles, nanocrystals and nanotubes. In recent years, biopolymer-based nanoparticles including protein nanoparticles are actively used in pharmaceuticals due to their low toxicity and biodegradability. They also have better biocompatibilities and the possibility for surface modification. These nanocarriers can be synthesized using proteins like albumin, gelatin, whey protein, gliadin, legumin, elastin, zein, soy protein and milk protein. These protein nanoparticles are an ideal material for delivery of bioactive compounds as their amphiphilic nature allows them to interact with both the bioactive compounds and the solvent. (Verma *et al*., 2018)

Albumin is an attractive macromolecule carrier due to its high binding capacity and is obtained from a variety of sources such as BSA, egg white (ovalbumin) and human serum albumin (HSA). It has a molecular weight of 66.5 kDa and is a water-soluble protein which is therefore used in maintaining the osmotic pressure, binding and transport of nutrients to the cells. Albumin also dissolves in ethanol (40% w/v), it is stable in the pH range of 4-9 and can be heated at 60 ℃ for 10 hours without showing any kind of denaturation effects. It is widely used in the preparation of nanospheres and nanocapsules as these albumin nanocarriers are non-toxic, biocompatible, biodegradable, easy to prepare, non-immunogenic, have well defined sizes and also carry some reactive groups such as thiols, amines and carboxyl. These groups can work as surface modifiers during the cross-linking process. Also, the bioactive compounds encapsulating albumin nanoparticles can be easily digested by the enzyme protease, releasing the entrapped material. Achieving the required particle size of albumin nanoparticles is easy and reproducible. (Verma *et al*., 2018; Amighi *et al*., 2020)

Albumin nanoparticles can be prepared by various techniques such as desolvation, emulsification, Nanoparticle Albumin-Bound (NAB) technology and nano-spray drying. (Amighi, *et al*., 2020). Among these methods, the most commonly used methods are desolvation and emulsification. (Niknejad & Mahmoudzadeh, 2015)

Under the desolvation method, a desolvation agent which is an organic solvent such as ethanol or acetone or even a natural salt is added into the aqueous solution of albumin. By adding desolvation agents, albumin starts to change its tertiary structure slowly. Then at a certain level, protein clumps (aggregates) are made and finally these unstable aggregates are hardened by the cross-linking agent. (Niknejad & Mahmoudzadeh, 2015) In order to separate the particles, the turbidity of the system should be increased. In the emulsification method, an aqueous phase of albumin is prepared with distilled water, which is added to an organic phase plant oil such as cotton seed oil under mechanical homogenizer until an oil-water emulsion is prepared. This emulsion is then added into preheated oil over 120 ∘C drop by drop. This results in evaporation of water and irreversible destruction of albumin which leads to the formation of nanoparticles. The resulting particles are then suspended in an ice-cold bath. (Verma *et al*., 2018)

BSA nanoparticles can be synthesized using the desolvation method, where ethanol can be used as the desolvation agent to obtain nanoparticles with narrower size distribution and controllable particle size. Cross-linking is an essential step in nanoparticle synthesis, as it influences bio-decomposability of the loaded bioactive compounds and their release from the nanocarrier system. A cross-linker is added to stabilize the newly formed nanoparticles. The addition of a cross-linking agent changes the surface charge of nanoparticles. Also, it modifies the colloidal stability and electrostatic potential of the BSA nanoparticles in solution. Recently, natural origin cross-linkers such as citric acid which guarantees human health have started to become very popular. During the cross-linking process of citric acid, more than one carboxyl group reacts with proteins. Also, citric acid starts its cross-linking process in alkaline pH values. At higher pH values, amino groups are deprotonated, so the free amino groups attack the partially positively charged carbonyl carbons of citric acid resulting in a nucleophilic substitution. (Amighi *et al*., 2020; Aniesrani Delfiya *et al*., 2016))

The objective of the present study was to synthesize and characterize ALNP, so that it could be used as an antidiabetic nutraceutical to treat hyperglycemia.

MATERIALS AND METHODS

Raw Materials

Alpinia calcarata rhizomes

Chemicals

BSA, Ethanol, Citric acid, Sodium hydroxide, Alpha amylase, Starch, Dinitrosallicylic acid reagent (DNS), Sodium hydrogen phosphate, Sodium dihydrogen phosphate, Dimethyl sulfoxide (DMSO), Anhydrous KBr, Baker's yeast and Anhydrous dextrose.

Instruments

Electric grinder (Sumeet, India), Analytical balance (Kern ALJ 120-4 Germany), Pressure cooker (Prestige India), Centrifuge machine, Magnetic stirrer, pH meter, Thermometer, Electric oven, Microplate reader (Spectra Max M5, Molecular Devices, CA, USA), Malvern Zetasizer Nano ZS apparatus (Malvern Instruments Ltd., Malvern, UK), Field emission scanning electron microscope (Hitachi SU6600 FE-SEM), UV-VIS spectrophotometer (Agilent Technologies, Germany. Cary 60), FT-IR (Fourier transform infrared) spectrometer (PerkinElmer, L 1600300 Spectrum TWO LITA, Liantrisant, UK).

Preparation of *Alpinia calcarata* powder

Dried *Alpinia calcarata* rhizomes grown in Sri Lanka were obtained and ground into fine powder using an electric grinder and refrigerated at -10 ℃ until further use.

Preparation of aqueous *Alpinia calcarata* extract

A. calcarata powder (10.00 g, < 0.5 mm) was digested using

distilled water (100.00 mL) under a pressure of 15 psi (121 ℃) for 15 minutes in medium pressure. The extract was filtered using a muslin cloth and the filtrate was centrifuged at 3000 rpm for 15 minutes. The supernatant obtained was then stored at -20 ℃ until further analysis.

Preparation of ALNP

For the synthesis of ALNP, an aqueous extract of *A. calcarata* (4.00 mL) was mixed with ethanol (16.00 mL) and added at a rate of 1.00 mL/min to a BSA solution (20 mg/mL, 4.00 mL, pH 9) while the solution was constantly stirring at 600 rpm at 4 ℃. Then citric acid (8% w/v, 230 µL) was added as the cross-linking agent, and the mixture was allowed to stir for another 2-3 hours, at 4 ℃. The mixture was then stored at 4 ℃ for 24 hours, for the formation of stable nanoparticles, by facilitating the cross-linking process. The nanoparticle bearing solution was centrifuged at 3000 rpm for 30 minutes and the pellet containing the nanoparticles was purified by five cycles of centrifugation (15000 g, 10 min) using Milli-Q water. The obtained particles were then dried at 50 ℃ until a constant weight was observed and then stored at 4 ℃ until further analysis.

Determining the yield of ALNP

Weight of the obtained product was measured. Total concentration of all compounds in *A.calcarata* extract was determined by evaporating *A.calcarata* extract (1.00 mL) on an evaporating glass and weighing the remaining. Using the obtained data, the yield was calculated according to the following equation.

Yield = (Weight of the product (g) /Weight of used BSA + Weight of *A.calcarata* extract)×100

Determining antidiabetic activity of ALNP

Antidiabetic activity of the aqueous *Alpinia calcarata* extract and ALNP were determined by carrying out in-vitro alpha amylase inhibition assay.

Alpha amylase inhibition assay

The alpha amylase inhibitory activity of aqueous *A.calarata* extract and ALNP were determined by following the method specified in Oyedemi, *et al.*, 2017 with slight modifications.

A concentration series (1 – 8 mg/mL) of the aqueous *A.calarata* extract was prepared. Each solution (500 µL) was placed in a separate Eppendorf tube. Alpha amylase enzyme (0.05 mg/mL, 250 µL) in sodium phosphate buffer (0.02 M, pH 6.9) was added to each Eppendorf tube. The mixtures were then incubated at room temperature (28 ± 2 ℃) for 15 minutes. Starch solution (1%, 250 µL) in sodium phosphate buffer (0.02 M, pH 6.9) was added. The reaction mixtures were incubated at room temperature (28 ± 2 ℃) for 15 minutes. DNS reagent (250 µL) was added to each Eppendorf tube, and all the tubes were boiled for 5 minutes. Absorbance was measured at 540 nm using the microplate reader. This procedure was triplicated.

Three more separate series were carried out, one where the enzyme was replaced with sodium phosphate buffer (0.02 M, pH 6.9, 250 µL), another where the aqueous *A.calcarata* extract was replaced with sodium phosphate buffer (0.02 M, pH 6.9, 500 µL) and another series where both the aqueous *A.calcarata* extract and the enzyme were replaced by sodium phosphate buffer (0.02 M, pH 6.9, 750 µL). Each of these series were also performed in triplicates.

Percentage inhibition of the alpha amylase enzyme was calculated using the following formula.

$$\text{Percentage inhibition (\%)} = \frac{(A - B) - (C - D)}{(A - B)} \times 100$$

A = Absorbance at 540 nm without inhibitor and with enzyme
B = Absorbance at 540 nm without inhibitor and enzyme
C = Absorbance at 540 nm with inhibitor and enzyme
D = Absorbance at 540 nm with inhibitor and without enzyme

Based on the percentage inhibition values, the IC50 value of the aqueous *A.calcarata* extract on alpha amylase enzyme was calculated using the GraphPad Prism 9.2.0 software.

Concentration series of ALNP (0.13 – 1.00 mg/mL) was prepared using DMSO as the solvent. The percentage inhibition and IC50 value of ALNP on alpha amylase enzyme was calculated using the same procedure that was followed for the aqueous *A.calcarata* extract.

Yeast glucose uptake assay

Glucose uptake by yeast cells in the presence of *A. calcarata* aqueous extract and ALNP were determined by following the method described by Cirillo, *et al.*, 1962 with slight modifications. A 1% yeast solution was prepared by dissolving commercial baker's yeast (0.25 g) in distilled water (0.25 mL) and was left overnight at room temperature. The following day, the solution was centrifuged at 4200 rpm for 5 min repeatedly until a clear supernatant was obtained. 10% (v/v) suspension was prepared in distilled water. Glucose solution (25 mM) was prepared by dissolving anhydrous glucose (0.45 g) in distilled water (100.0 mL). Then using the prepared glucose solution, 10 mM and 5 mM glucose concentrations were prepared by diluting with distilled water. A concentration series of *A. calcarata* aqueous extract (0.48 – 7.60 mg/mL) as well as a concentration series of ALNP (0.03 – 0.54 mg/mL) were prepared by using distilled water and DMSO as solvents, respectively. The extract (1.00 mL) and nanoparticle suspension (1.00 mL) were added separately to glucose solution (5 mM, 10 mM, and 25 mM, 1.00 mL) and incubated at 37 °C for 10 min. Then the yeast suspension (100 µl) was added to start the reaction, and the mixtures were vortexed and further incubated at 37 ℃ for 60 min. The tubes were then centrifuged (2500 g, 5 min) and glucose in the supernatant was estimated by adding DNS reagent (250 µl) to supernatant (1.00 mL) and the mixtures were boiled for 5 min. Absorbance was measured at 540 nm by microplate reader. Blank was prepared by adding distilled water (300 µl) instead of the sample solution.

The procedure was triplicated. The percentage increase in glucose uptake by yeast cells was calculated using the following formula.

$$\text{Percentage increase in glucose uptake (\%)} = \frac{A_{control} - A_{sample}}{A_{control}} \times 100$$

Characterization of ALNP

Solubility

ALNP (5.0 mg) was added to distilled water (5.00 mL) and stirred for 30 minutes at 600 rpm at room temperature. After that the mixture was centrifuged at 10 000 rpm for 15 minutes. Pellet was dried at 100 °C in an oven until a constant weight was observed. The procedure was triplicated. The solubility was calculated according to the following formula.

$$\text{Solubility (\%)} = \frac{\text{Weight of the product added (g) - Weight of the pellet (g)}}{\text{Weight of the product added (g)}} \times 100$$

***A.calcarata* loading and entrapment efficiency**

A concentration series from the pressured water extract of *A.calcarata* was prepared. Absorbance of the concentration series was measured at 310 nm. A graph of absorbance at 310 nm vs concentration of *A.calcarata* extract was plotted (Attieh, *et al*., 2015). Absorbance of the supernatants which remained after the separation of the product containing pellet, was measured at 310 nm. By comparing the absorbance value of the supernatant with the standard curve, the concentration of remaining *A.calcarata* compounds in the supernatant was found. The procedure was triplicated. *A.calcarata* loading and entrapment efficiencies were determined by using following formulae.

Weight of *A.calcarata* loaded = Weight of *A.calcarata* added - Weight of *A.calcarata* in supernatant

$$A.calcarata \text{ loading (\%)} = \frac{\text{Weight of } A.calcarata \text{ loaded}}{\text{Total weight of the product}} \times 100$$

$$A.calcarata \text{ entrapment efficiency (\%)} = \frac{\text{Weight of } A.calcarata \text{ loaded}}{\text{Weight of } A.calcarata \text{ added}} \times 100$$

Determination of particle size and zeta potential

The particle size, PDI and zeta potential of the ALNP were determined with the Malvern Zetasizer Nano ZS apparatus. An aqueous suspension of ALNP was diluted 1:100 with ultrapure water and the solution was placed in a disposable polystyrene cuvette and the particle size measurement was obtained. The solution was also placed in a folded capillary zeta cell and the zeta potential measurement was obtained. Both procedures were triplicated.

Morphological observations

Field emission scanning electron microscope was used to visualize the morphology and shape of the synthesized ALNP. The sample was mounted onto the sample stub using carbon tapes and the images were taken after gold sputter coating for 15 seconds.

UV-visible absorbance spectra

The UV-visible absorption spectra were analyzed using a UV-visible spectrophotometer from 200 to 500 nm within a 1 cm quartz cell. A 0.8 mg/mL synthesized ALNP sample was prepared after dissolving it in DMSO and its absorbance spectrum was obtained. It was then compared with the absorbance spectra of 1 mg/mL pure BSA, 0.07 mg/mL aqueous *A.calcarata* extract and 0.8% w/v citric acid. The absorbance spectrum of distilled water was subtracted from all sample spectra.

FT-IR spectroscopy

The molecular characteristics of the ALNP were examined and compared with that of pure BSA, oven dried aqueous *A.calcarata* extract and pure cross-linking agent, citric acid using an FT-IR spectrometer. Each sample was mixed with anhydrous KBr in a 1:10 ratio and ground using a motor and pestle until a fine powder was obtained. A small portion of the powder was placed in the pellet forming mold and pressed under pressure. Then the pellet was placed in the FT-IR spectrometer and scanned in the wavenumber range of 750-4000 cm-1.

Statistical Analysis

The obtained data were statistically analyzed by one-way analysis of variance (ANOVA) using Minitab software package. The results were expressed in the form of mean ± standard deviation of triplicate determinants. The level of significance was taken at 5% confidence interval ($p < 0.05$).

RESULTS

Physical appearance of ALNP

Table 1: Yield and morphology of ALNP

Yield (%)	Morphology
94.11	Light brown coloured powder

Antidiabetic activity

Alpha amylase inhibition assay

Table 2: IC_{50} values of alpha amylase enzyme

Sample	IC_{50} value on alpha amylase enzyme (µg/mL)
Aqueous *A.calcarata* extract	152.10 (±0.10) [a]
ALNP	147.00 (±0.97) [b]

Means followed by different letters are significantly different ($p < 0.05$)

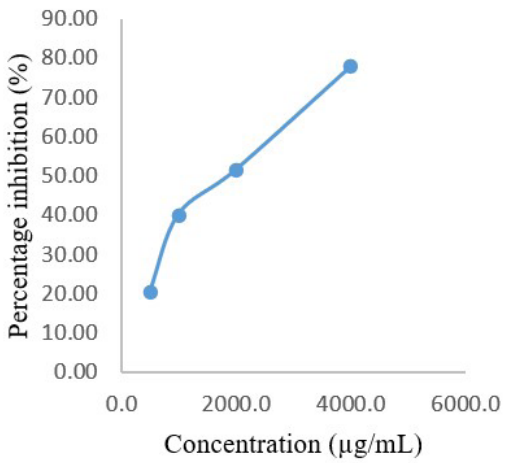

Figure 1 : The graph of percentage inhibition (%) of aqueous *A.calcarata* extract on alpha amylase enzyme vs. concentration

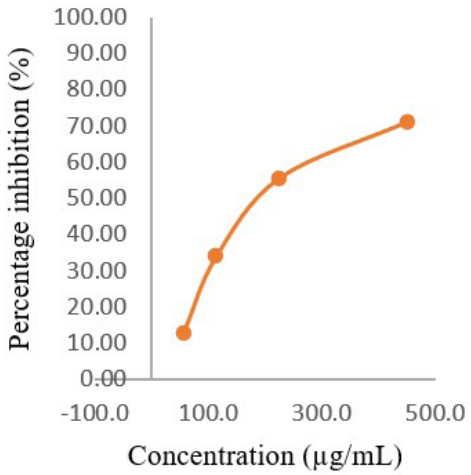

Figure 2 : The graph of percentage inhibition (%) of ALNP on alpha amylase enzyme vs. concentration

Yeast glucose uptake assay

Table 3 : Percentage increase in glucose uptake by yeast cells at different glucose concentrations in the presence of aqueous *A.calcarata* extract

Concentration(mg/mL)	Glucose uptake percentage (%) at different glucose concentrations		
	5 mM	10 mM	25 mM
7.6	68.66 (±0.02) [a]	43.57 (±0.26) [a]	24.20 (±2.02) [a]
3.8	64.61 (±0.29) [b]	32.28 (±0.26) [b]	22.22 (±0.13) [ab]
1.9	58.45 (±0.34) [c]	20.68 (±0.91) [c]	20.20 (±0.39) [b]
0.95	50.78 (±0.07) [d]	17.14 (±0.47) [d]	16.69 (±0.16) [c]
0.475	45.30 (±0.97) [e]	15.23 (±0.40) [e]	14.16 (±0.30) [d]

Means followed by different letters are significantly different ($p < 0.05$)

Table 4 : Percentage increase in glucose uptake by yeast cells at different glucose concentrations in the presence of ALNP

Concentration(mg/mL)	Glucose uptake percentage (%) at different glucose concentrations		
0.54	73.09 (±0.06) a	49.81 (±0.09) a	28.89 (±0.56) a
0.27	71.28 (±0.52) b	38.41 (±0.28) b	26.82 (±0.88) b
0.135	68.97 (±0.80) c	31.66 (±0.40) c	24.82 (±0.76) c
0.0675	64.17 (±0.16) d	25.38 (±0.72) d	20.97 (±0.87) d
0.03375	60.80 (±0.70) e	18.03 (±0.82) e	16.63 (±0.35) [e]

Means followed by different letters are significantly different ($p < 0.05$)

Characterization of ALNP

Table 5 : Solubility, *A.calcarata* loading percentage and *A.calcarata* entrapment efficiency of ALNP

Solubility in water (%)	A.calcarata loading percentage (%)	A.calcarata entrapment efficiency (%)
64.00 (±1.00)	6.66 (±0.01)	87.71 (±0.07)

Table 6 : Particle size, PDI and zeta potential of ALNP

Parameter	Mean ± Standard deviation
Particle size	1030.70 (±75.3) nm
PDI	0.199 (± 0.003)
Zeta potential	2.57 (±0.32) mV

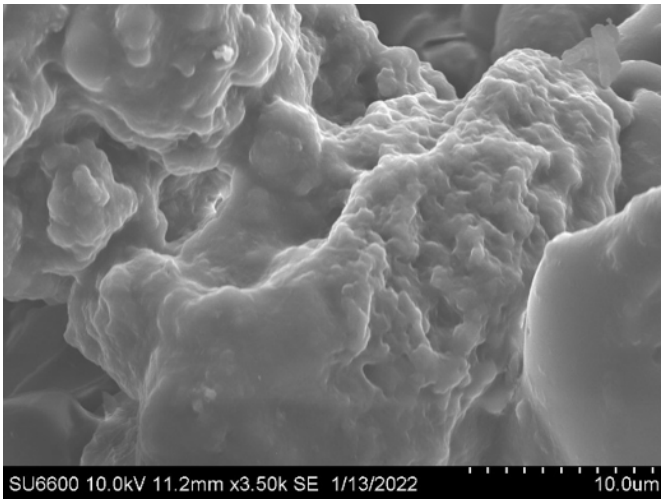

Figure 3: SEM image of ALNP

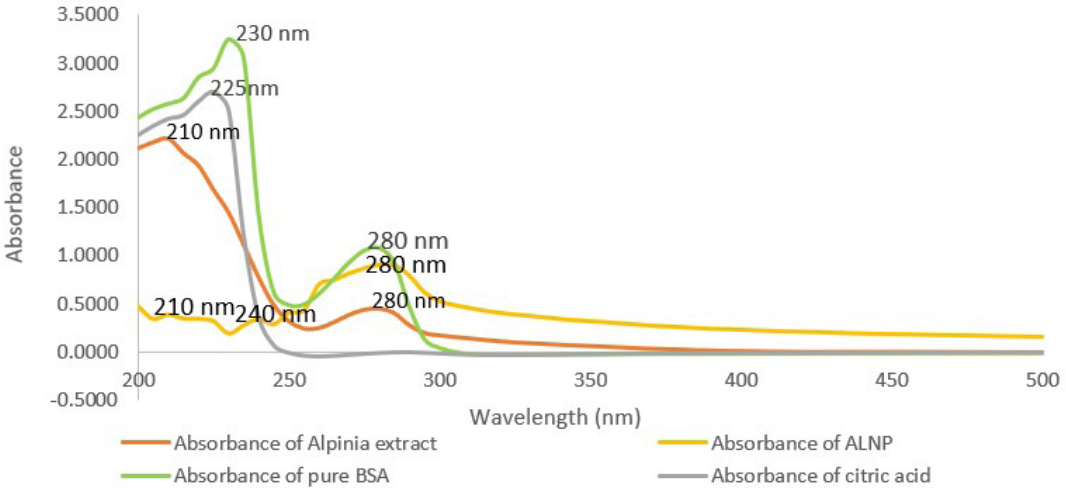

Figure 4 : UV-Visible absorbance spectra of pure BSA, aqueous *A.calcarata* extract, pure citric acid and ALNP

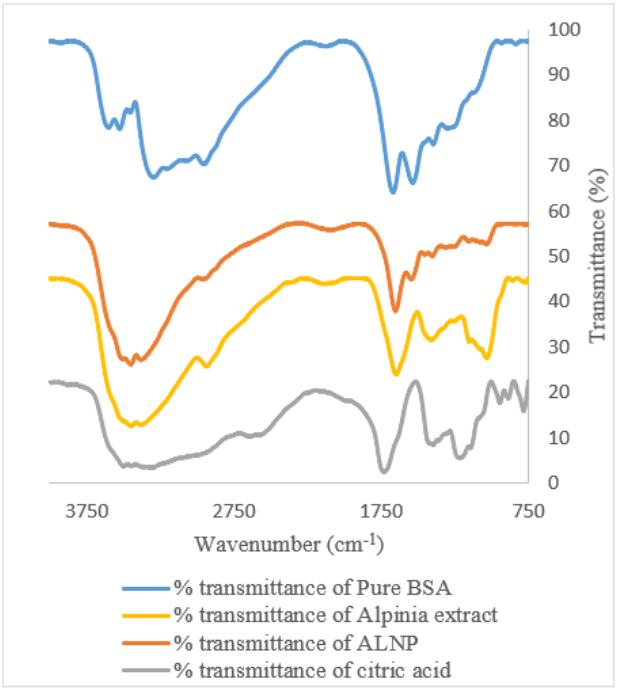

Figure 5 : FT-IR spectra of pure BSA, aqueous *A.calcarata* extract, pure citric acid and ALNP

DISCUSSION

As the rhizome extract of Sri Lankan *Alpinia calcarata* has shown potential antidiabetic effects, its pressured water extract was used to synthesize nanoparticles, in order to be used as an antidiabetic nutraceutical. (Samarasinghe, *et al.*, 2020) Nanoparticles were synthesized using its extract in order to increase the solubility of its bioactive compounds while allowing specific delivery and controlled release to target sites with reduced side effects and prolonged shelf-life. (Assadpour & Mahdi Jafari, 2019; Paolino *et al.*, 2021) The synthesized ALNP appeared in powder form (Table 1). When compared to the conventional microencapsulated products obtained from techniques such as spray drying and freeze drying, these powder form nanocarriers provide more bioavailability through increased surface-to-volume ratio providing them the ability to easily pass through the cell membranes and penetrate into target cells releasing their encapsulated compounds. (Assadpour & Mahdi Jafari, 2019) The obtained colour of the ALNP should be due to the entrapment of the bioactive compounds of the extract within the synthesized nanocarriers. As a high concentration of BSA was used during the nanoparticle synthesis, a high yield of 94.11% of ALNP was recorded. (Aniesrani *et al.*, 2016)

IC50 values of aqueous A .calcarata extract and ALNP are given in in table 2. When comparing the IC50 values, it can be seen that the synthesized ALNP showed a higher alpha amylase inhibitory activity than the crude *A. calcarata* extract. This proves that the antidiabetic activity of bioactive compounds becomes much higher when loaded onto nanocarriers probably due to the increased surface area to volume ratio resulting in a higher feasibility of interacting with the alpha amylase enzyme.

The percentage increase in glucose uptake by yeast cells in the presence of aqueous *A.calcarata* extract and ALNP are given in table 3 and table 4 respectively. The glucose uptake by yeast cells is indicated by the change in glucose concentration in the medium after a particular time interval. The aqueous *A.calcarata* extract as well as ALNP have promoted the uptake of glucose across the plasma membrane of yeast cells according to tables 3 and table 4 respectively. However, the glucose uptake capacity at approximately 0.5 mg/mL aqueous extract was 45.30 (±0.97) %, and for that of synthesized ALNP was 73.09 (±0.06) %, for the 5mM glucose concentration. Similarly, the ALNP exhibited a higher activity than the aqueous extract at all glucose concentrations used in the study. Therefore, this once again proves that the antidiabetic activity of the aqueous extract becomes further enhanced when going into the nanoscale. Moreover, the glucose uptake capacity at 0.03 mg/mL of ALNP was 60.80 (±0.70) % and that has reached up to 73.09 (±0.06) % when 0.5 mg/mL of ALNP was used, in the presence of a 5 mM glucose concentration. This means that by increasing the nanoparticle concentration, the capability of yeast cells to uptake more glucose from the environment can be increased. A similar increment in the glucose uptake capacity was observed when 10 mM and 25 mM glucose concentrations were used. However, an inverse relationship to the molar concentration of glucose was observed with the percent increase in glucose uptake by yeast cells, when 5 mM, 10 mM and 25 mM glucose concentrations were compared for the same amount of ALNP. From the results it is clear that lower the glucose concentration, higher the uptake by yeast cells. This observation is in good agreement with the earlier work of Rehman, *et al.*, 2018 and Bhutkar, *et al.*, 2016.

The solubility of ALNP in water is given in table 5. Solubility of the ALNP is determined by the pH of the BSA solution as it affects the size of the nanoparticles formed. The isoelectric point of BSA is around 4.7. Hence, at pH 9 the BSA protein molecules are ionized and therefore they tend to repulse each other. This causes the synthesized ALNP to become smaller and smaller, increasing their surface area and thereby resulting in greater solubility in water. Table 5 also shows the *A. calcarata* loading percentage and *A. calcarata* entrapment efficiency of the ALNP. During nanoparticle synthesis, as the BSA concentration that was used was high (20 mg/mL), it may have increased the number of nanoparticles that were formed. When the quantity of nanoparticles is higher, it will decrease the amount of *A. calcarata* that gets loaded with constant addition. Also, the high pH of the BSA solution (pH 9) will also decrease the amount of *A. calcarata* that gets loaded due to the high electrostatic repulsion between BSA and *A.calcarata*. This explains the small value for the *A. calcarata* loading percentage of the synthesized ALNP. Also, a high BSA concentration will increase the entrapment efficiency as larger particles have larger volumes which increases the quantity of *A. calcarata* that can be held by the synthesized ALNP. This explains the high value obtained for the *A.calcarata* entrapment efficiency of ALNP. (Aniesrani *et al.*, 2016; Ranasinghe, *et al.*, 2013)

ALNP showed a mean diameter of 1030.70 (±75.3) nm (Table 6). According to Amighi, *et al.*, 2020, the nanoparticle size that is obtained under the conditions that were used in ALNP synthesis with citric acid as the cross-linking agent is 1201.00 (±58.4) nm. As the mean particle size obtained for ALNP is very close to this value, it is clear that these nanoparticles have been formed effectively.

According to Danaei, *et al.*, 2018, the PDI of a nanoparticle sample with effective particle size distribution should be between 0.05-0.7. As the PDI value of ALNP falls within this range, it can be stated that a homogenous population of nanocarriers have been synthesized, which can act as safe, stable and efficient nanocarriers of *A. calcarata*. Therefore, the tendency of this antidiabetic nutraceutical to accumulate in the target tissue, which depends on the particle size distribution will be minimal.

Nanoparticles with a zeta potential between -10 and +10 mV are considered neutral, while nanoparticles with zeta potentials greater than +30 mV are considered strongly cationic and those with zeta potentials less than -30 mV are considered strongly anionic. Since most cell membranes

are negatively charged, zeta potential can strongly affect a nanoparticle's tendency to penetrate membranes, with cationic particles displaying toxicity due to cell membrane disruption. (Clogston & Patri, 2011) As the zeta potential of ALNP is 2.57 (±0.32) mV, these nanoparticles are neutral and will be able to easily penetrate the cell membranes without causing any toxicological effects. This further ensures that the synthesized ALNP can be effectively used as an antidiabetic nutraceutical.

The morphological analysis of ALNP was carried out with FE-SEM, and the obtained image is shown in figure 3. The SEM micrograph obtained revealed morphological aspects of ALNP with a spherical shape and uniform size. When comparing the UV-visible absorbance spectrum of ALNP with that of the aqueous *A.calcarata* extract, peaks at 210 nm and 280 nm were observed in both spectra (Figure 4). This means that the active compounds of *A. calcarata* have been successfully loaded into the BSA nanoparticles. Therefore, this proves that the active compounds of the aqueous *Alpinia calcarata* extract have been successfully loaded into the BSA nanoparticles. However, a peak corresponding to citric acid was not observed in the UV absorbance spectrum of the *A. calcarata* loaded nanoparticles. This means that citric acid was completely washed away during the washing step performed in the purification of nanoparticles. The pure BSA spectrum showed a characteristic peak at 280 nm. Therefore, the peak observed at 280 nm in the ALNP spectrum may be due to both BSA and the active compounds of *A. calcarata*.

When considering the FT-IR spectrum of ALNP, it too showed peaks that could also be observed in the FT-IR spectrum of the aqueous Alpinia extract (Figure 5). Characteristic peaks including =C-H stretch at 3300 cm-1, C=C benzene stretch of two peaks between 1400-1600 cm-1 and OH stretch by a broad peak between 3000-3600 cm-1 were observed in both spectra. Therefore, this gives further evidence for the successful entrapment of the *A.calcarata* compounds within the synthesized ALNP. According to Xu, *et al*., 2015, one to two carboxyl groups of one citric acid molecule can react with BSA, resulting in an increase in the total amount of carboxyl groups and a decrease in the total amount of amine groups in the cross-linked nanoparticles. This explains the presence of a peak corresponding to the OH stretch and decrease in intensity of the peak at 3400 cm-1 corresponding to the N-H stretch in the spectrum of ALNP. This means that interactions between BSA and citric acid have caused conformational changes in the protein structure of the synthesized nanoparticles. A similar observation has been made by Amighi, *et al*., 2020 during the synthesis of BSA nanoparticles using citric acid as the cross-linking agent. Furthermore, two peaks at 1665 cm-1 and 1537 cm-1 were observed in the pure BSA spectrum corresponding to the Amide I and Amide II stretches respectively. However, in the ALNP spectrum the peak corresponding to the Amide I stretch was absent and a noticeable shift was seen in the peak corresponding to the Amide II stretch. Hence, loading of *A. calcarata* compounds have also induced conformational changes in the structure of the BSA protein. This means that the active compounds of *A. calcarata* have interacted with the protein matrix of the synthesized nanoparticles via covalent bonds. This result is similar to the results obtained by Rani, 2016.

CONCLUSION

The present study has proven that the antidiabetic activity of bioactive compounds of *Alpinia calcarata* becomes enhanced when loaded onto nanocarriers. A high yield of 94.11% of ALNP were synthesized which appeared in powder form, had a spherical morphology, uniform size, with effective particle size distribution and a neutral surface charge. As the BSA solution used had a pH value of 9, which was further away from its isoelectric point, ALNP reported a solubility percentage of 64%. A high *A. calcarata* entrapment efficiency of 87.71% and an *A.calcarata* loading percentage of 6.66% were also recorded for the synthesized nanoparticles. The mean particle size of the ALNP was 1030.70 nm. The FT-IR spectrum of nanoparticles showed that the cross-linking agent, citric acid had caused conformational changes in the protein structure of BSA and that the active compounds were successfully loaded into the synthesized nanoparticles which interacted with the protein matrix via covalent bonds. The UV-visible absorbance spectrum of ALNP further proved the successful entrapment of the active *A. calcarata* compounds within the nanoparticles and also showed that citric acid was completely washed away during the washing step. Therefore, it can be concluded that ALNP have been synthesized effectively, which can be used as a powder form antidiabetic nutraceutical. A limitation of this study was the high particle size obtained for the synthesized ALNP and therefore future work can be carried out to reduce it by testing various other desolvation agents and cross-linking agents. Also, in-vivo antidiabetic analysis can be carried out to test the effect of the synthesized ALNP within living organisms in the future.

Acknowledgements

This study was funded by the University Grant RP/03/02/06/01/2021 which is gratefully acknowledged.

Conflict of interest

There is no conflict of interest.

REFERENCES

Amighi, F., Emam-Djomeh, Z., & Labbafi-Mazraeh-Shahi, M. (2020). Effect of different cross-linking agents on the preparation of bovine serum albumin nanoparticles. *Journal of the Iranian Chemical Society, 17*(5), 1223–1235. https://doi.org/10.1007/s13738-019-01850-9

Aniesrani Delfiya, D. S., Thangavel, K., & Amirtham, D. (2016). Preparation of Curcumin Loaded Egg Albumin Nanoparticles Using Acetone and

Optimization of Desolvation Process. *The Protein Journal, 35*(2), 124–135. https://doi.org/10.1007/s10930-016-9652-3

Arambewela, L. S. R., Kumaratunge, A., Arawwawela, M., Owen, N. L., & Du, L. (2005). Volatile Oils of *Alpinia calcarata* Rosc. Grown in Sri Lanka. *Journal of Essential Oil Research, 17*(2), 124–125. https://doi.org/10.1080/10412905.2005.9698850

Assadpour, E., & Mahdi Jafari, S. (2019). A systematic review on nanoencapsulation of food bioactive ingredients and nutraceuticals by various nanocarriers. *Critical Reviews in Food Science and Nutrition, 59*(19), 3129–3151. https://doi.org/10.1080/10408398.2018.1484687

Assadpour, E., & Mahdi Jafari, S. (2019). A systematic review on nanoencapsulation of food bioactive ingredients and nutraceuticals by various nanocarriers. *Critical Reviews in Food Science and Nutrition, 59*(19), 3129–3151. https://doi.org/10.1080/10408398.2018.1484687

Attieh, H. A., Abu Lafi, S., Jaber, S., Abu-Remeleh, Q., Lutgen, P., & Akkawi, M. (2015). Cinnamon bark water-infusion as an in-vitro inhibitor of β-hematin formation. https://dspace.alquds.edu/handle/20.500.12213/1023

Bhutkar, M. A., Bhinge, S. D., Randive, D. S., & Wadkar, G. H. (2017). Hypoglycemic effects of Berberis aristata and Tamarindus indica extracts in vitro. *Bulletin of Faculty of Pharmacy, Cairo University, 55*(1), 91–94. https://doi.org/10.1016/j.bfopcu.2016.09.001

Cirillo, V. P. (1962). Mechanism of glucose transport across the yeast cell membrane. *Journal of Bacteriology, 84*(3), 485–491. https://www.ncbi.nlm.nih.gov/pmc/articles/PMC277903/

Clogston, J. D., & Patri, A. K. (2011). Zeta potential measurement. *Methods in Molecular Biology (Clifton, N.J.), 697,* 63–70. https://doi.org/10.1007/978-1-60327-198-1_6

Danaei, M., Dehghankhold, M., Ataei, S., Hasanzadeh Davarani, F., Javanmard, R., Dokhani, A., Khorasani, S., & Mozafari, M. R. (2018). Impact of Particle Size and Polydispersity Index on the Clinical Applications of Lipidic Nanocarrier Systems. *Pharmaceutics, 10*(2), 57.https://doi.org/10.3390/pharmaceutics10020057

Fourier Transform Infrared Spectroscopy (FTIR) Spectral Analysis of BSA Nanoparticles (BSA NPs) and Egg Albumin Nanoparticles (EA NPs). (2016). *Research Journal of Chemical Sciences, 6*(2), 29–36. http://www.isca.in/rjcs/Archives/v6/i2/5.ISCA-RJCS-2016-006.php

Guthrie, R. A., & Guthrie, D. W. (2004). Pathophysiology of diabetes mellitus. *Critical Care Nursing Quarterly, 27*(2), 113–125. https://doi.org/10.1097/00002727-200404000-00003

Hanadi, A. A., Saleh, A. L., Suhair, J., Qassem, A. R., Pierre, L., & Mutaz, A. (2015). Cinnamon bark water-infusion as an in-vitro inhibitor of -hematin formation. *Journal of Medicinal Plants Research, 9*(38), 998–1005. https://doi.org/10.5897/JMPR2015.5931

Jayawardena, B., & Smith, R. M. (2010). Superheated water extraction of essential oils from Cinnamomum zeylanicum (L.). *Phytochemical Analysis: PCA, 21*(5), 470–472. https://doi.org/10.1002/pca.1221

Kazeem, M. I., & Davies, T. C. (2016). Anti-diabetic functional foods as sources of insulin secreting, insulin sensitizing and insulin mimetic agents. *Journal of Functional Foods, 20,* 122–138. https://doi.org/10.1016/j.jff.2015.10.013

Kerner, W., Brückel, J., & German Diabetes Association. (2014). Definition, classification and diagnosis of diabetes mellitus. Experimental and Clinical Endocrinology & Diabetes: *Official Journal, German Society of Endocrinology German Diabetes Association, 122*(7), 384–386. https://doi.org/10.1055/s-0034-1366278

Kharroubi, A. T., & Darwish, H. M. (2015). Diabetes mellitus: The epidemic of the century. *World Journal of Diabetes, 6*(6), 850–867. https://doi.org/10.4239/wjd.v6.i6.850

Niknejad, H., & Mahmoudzadeh, R. (2015). Comparison of Different Crosslinking Methods for Preparation of Docetaxel-loaded Albumin Nanoparticles. Iranian *Journal of Pharmaceutical Research : IJPR, 14*(2), 385–394. https://www.ncbi.nlm.nih.gov/pmc/articles/PMC4403054/

Oyedemi, S. O., Oyedemi, B. O., Ijeh, I. I., Ohanyerem, P. E., Coopoosamy, R. M., & Aiyegoro, O. A. (2017). Alpha-Amylase Inhibition and Antioxidative Capacity of Some Antidiabetic Plants Used by the Traditional Healers in Southeastern Nigeria. *The Scientific World Journal, 2017,* 3592491. https://doi.org/10.1155/2017/3592491

Paolino, D., Mancuso, A., Cristiano, M. C., Froiio, F., Lammari, N., Celia, C., & Fresta, M. (2021). Nanonutraceuticals: The New Frontier of Supplementary Food. *Nanomaterials (Basel, Switzerland), 11*(3), 792. https://doi.org/10.3390/nano11030792

Rahman, M. A., & Islam, M. S. (2015). *Alpinia calcarata* Roscoe: A potential phytopharmacological source of natural medicine. *Pharmacognosy Reviews, 9*(17), 55–62. https://doi.org/10.4103/0973-7847.156350

Rahman, M. A., & Islam, M. S. (2015). *Alpinia calcarata* Roscoe: A potential phytopharmacological source of natural medicine. *Pharmacognosy Reviews, 9*(17), 55–62. https://doi.org/10.4103/0973-7847.156350

Ranasinghe, P., Pigera, S., Premakumara, G. A. S., Galappaththy, P., Constantine, G. R., & Katulanda, P. (2013). Medicinal properties of "true" cinnamon (Cinnamomum zeylanicum): A systematic review. *BMC Complementary and Alternative Medicine, 13,* 275. https://doi.org/10.1186/1472-6882-13-275

Rehman, G., Hamayun, M., Iqbal, A., Ul Islam, S., Arshad, S., Zaman, K., Ahmad, A., Shehzad, A., Hussain, A., & Lee, I. (2018). In Vitro Antidiabetic Effects and Antioxidant Potential of Cassia nemophila Pods. *BioMed Research International, 2018,* e1824790. https://

doi.org/10.1155/2018/1824790

Samarasinghe, B., Kaliyadasa, E., & Marasinghe, P. (2020). Physicochemical Properties and Bioactivities of Six Alpinia Species in Sri Lanka. *International Journal of Ayurvedic Medicine, 11*(4). https://doi.org/10.47552/ijam.v11i4.1717

Sapra, A., & Bhandari, P. (2022). Diabetes Mellitus. In StatPearls. StatPearls Publishing. http://www.ncbi.nlm.nih.gov/books/NBK551501/

Teo, C. C., Tan, S. N., Yong, J. W. H., Hew, C. S., & Ong, E. S. (2010). Pressurized hot water extraction (PHWE). *Journal of Chromatography A, 1217*(16), 2484–2494. https://doi.org/10.1016/j.chroma.2009.12.050

Verma, D., Gulati, N., Kaul, S., Mukherjee, S., & Nagaich, U. (2018). Protein Based Nanostructures for Drug Delivery. *Journal of Pharmaceutics, 2018,* 9285854. https://doi.org/10.1155/2018/9285854

Wariyapperuma, W. A. N. M., Kannangara, S., Wijayasinghe, Y., Subramanium, S., & Jayawardena, B. (2018). Pressured water extraction and solvent extraction of Cinnamomum zeylanicum (L.) bark and evaluation of anti-diabetic properties.

Wasana, K. G. P., Attanayake, A. P., Jayatilaka, K. A. P. W., & Weerarathna, T. P. (2021). Antidiabetic Activity of Widely Used Medicinal Plants in the Sri Lankan Traditional Healthcare System: New Insight to Medicinal Flora in Sri Lanka. *Evidence-Based Complementary and Alternative Medicine, 2021,* e6644004. https://doi.org/10.1155/2021/6644004

Xu, H., Shen, L., Xu, L., & Yang, Y. (2015). Controlled delivery of hollow corn protein nanoparticles via non-toxic crosslinking: In vivo and drug loading study. *Biomedical Microdevices, 17*(1), 8. https://doi.org/10.1007/s10544-014-9926-5